Role of boundary conditions in the finite-size Ising model

G. G. Cabrera
*Laboratoire de Physique des Solides, Bâtiment 510, Université de Paris-Sud, Centre d'Orsay, 91405 Orsay, France and Instituto de Física "Gleb Wataghin," Universidade Estadual de Campinas (UNICAMP), Caixa Postal 6165, Campinas 13.081, São Paulo, Brazil**

R. Jullien
Laboratoire de Physique des Solides, Bâtiment 510, Université de Paris-Sud, Centre d'Orsay, 91405 Orsay, France
(Received 17 October 1986)

Boundary conditions monitor the finite-size dependence of scaling functions for the Ising model. We study the low-temperature phase for the extremely anisotropic limit, or quantum version of the 2D classical Ising model, by means of combined exact results and large-size numerical calculations. The mass gap (inverse of correlation length) is the suitable order parameter for the finite system, and its finite-size behavior is studied as a function of variable boundary conditions. We find that the well-known exponential convergence to zero of the mass gap is only valid in a limited range of parameters; it strikingly changes into a power law for antiperiodic boundary conditions. We suggest that this puzzling phenomenon is associated with topological excitations.

I. INTRODUCTION

Finite-size scaling effects are on the verge of being tested experimentally, especially in the field of magnetic superlattices, where ultrachain magnetic layers have been grown by molecular-beam-epitaxy techniques.[1] We may expect in the near future the appearance of systems where finite-size effects are within experimental resolution. One point which makes a quantitative test of the theory extremely difficult in real systems is the role played by the boundary conditions (BC's). This fact has been already noted by Barber and Fisher,[2] who explicitly studied the dependence of scaling functions on different boundary conditions for the spherical model (see also a recent review by Barber[3]).

With regards to quantum systems, the influence of BC's on finite-size scaling has been studied for the Ising chain in a transverse field.[4,5] While Burkhardt and Guim limit themselves to periodic, free, and antiperiodic BC's at criticality,[4] the present authors have made a thorough calculation *our of criticality* in the presence of gradually tunable BC's. In this paper we present some details of our calculation whose preliminary results were reported in a Letter.[5]

Quantum systems which are Hamiltonian versions of classical lattice models deserve special attention because of the fact that both exhibit the same critical behavior.[6] The Ising chain with transverse field is the quantum version of the classical two-dimensional (2D) Ising model. It can be considered as the extremely anisotropic limit of the 2D model when the reduced coupling constant K_1, along the time direction, and K_2, along the transverse spatial direction, go to infinity and zero, respectively,

$$K_1 \to \infty, \quad K_2 \to 0 \ . \tag{1}$$

In order to maintain criticality and the same physics, the lattice is correspondingly distorted, by being squeezed along the time direction, and the following constraint has to be satisfied:

$$K_2 \exp(2K_1) = \gamma^{-1} \ . \tag{2}$$

The product of the left-hand side of (2) is always finite and defines the transverse field γ (in reduced units). At the end of this limit process, thermal fluctuations have been replaced by quantum fluctuations induced by the transverse field. BC's are correspondingly mapped onto the quantum chain problem. It is worth remarking that we can visualize the above process as taking the continuous limit along the time direction (since the time lattice constant goes to zero), which implies that the finite quantum chain is equivalent to the classical 2D Ising model for infinitely extended strips of finite width (also called the cylinder geometry). Regular periodic boundary conditions are then assumed along the infinite time direction while different BC's are imposed for the finite spatial direction.

The so-called mass gap (the energy difference between the first excited state and the ground state) is the quantum counterpart of the inverse of the correlation length of classical systems.[6] For the infinite quantum chain the mass gap vanishes at the critical point (while the correlation length diverges) with a critical exponent, indicating the presence of massless-particle excitations.

The scaling hypothesis assumes that the correlation length is the only characteristic length of the problem near the critical point. Exactly at the critical point the correlation length diverges and consequently the properties of the system are invariant under a scale transformation.[7] The so-called finite-size scaling (FSS) technique calculates the properties of an infinite system from extrapolation of exact results for finite or semi-infinite geometries. Universality of second-order phase transitions allows for a quite accurate calculation of critical exponents by this method, which is also known as phenomenological renormalization.[8,9]

For first-order phase transitions no universality is *a priori* expected, since the correlation length remains finite during the transition and the microscopic details of the interactions cannot be forgotten. It can be shown however that the finite-size rounding of first-order transitions is nevertheless universal[10–12] as a result of the fact that the correlation length of finite systems, below the critical temperature, is much larger than the bulk correlation length.

The universality of scale functions, whether at criticality or not, is affected by the choice of BC's. At the critical point this has been explicitly calculated by Barber and Fisher for the spherical model,[2] and by Burkhardt and Guim for the quantum Ising chain.[4] This latter result using FSS agrees with the prediction of Cardy based on conformal invariance of correlation functions.[13]

The effects of different BC's out of criticality have been reported previously by the present authors[5] using as an example the finite-size dependence of the mass gap for the quantum Ising chain. In this paper we show the details of our calculation, which combines exact analytical results and very accurate large-size numerical calculations. The precise knowledge of the size dependence for the mass gap is extremely important, since it drives the size dependence of many other quantities, as long as the system is *not* at criticality. In particular, it has been shown that finite-size rounding of the magnetization near a first-order transition is closely related to the mass-gap behavior.[10,12] The following question is then posed. How universal is this latter dependence? The main conclusion of the present work can be stated as a warning: Universality arguments must be taken with special care when dealing with FSS. Some details, such as the choice of different BC's, can drastically change the scaling law which controls the way the system approaches the thermodynamic limit when it increases its size.

Concerning the one-dimensional quantum Ising model, the exact solution for the infinite chain has been found by Pfeuty,[14] while Hamer and Barber[15] have studied the mass-gap behavior for the finite chain with periodic boundary conditions. In this latter work numerical finite-size calculations for the mass gap have been compared with the exact solution for finite chains (in the high-temperature regime or disordered phase), showing the efficiency of FSS for this kind of problem.

Our present treatment is similar to the one followed in Ref. 4, where one transforms to a free-fermion problem via the Jordan-Wigner transformation.[16] For large finite-size calculations this appears to be an essential step, for it reduces the dimensionality 2^N of the original problem to N, where N is the number of spins in the chain.

For periodic BC's it is well known that the mass-gap varies exponentially with size.[10–12,15,17] When the correspondence with classical systems is made, the two low-lying quantum states are associated with the two largest eigenvalues of the transfer matrix for the 2D classical lattice model. The word "gap" is commonly used to describe both situations. In 1969, Fisher addressing the question of the asymptotic degeneracy of those eigenvalues below the bulk critical temperature, stated that on the basis of "general arguments" one can say that they are exponentially degenerate with size[17] (for the case of the strip geometry with periodic BC's). This exponential degeneracy seems to be universal for models which present a discrete broken symmetry such as Ising-like systems, the Potts model, etc.

We will show here that the above exponential degeneracy has a limited range of validity. It changes into a power law for antiperiodic BC's, thus illustrating the weakness of the concept of universality in this kind of problem.

Our problem is planned as follows. In Sec. II we discuss briefly the Wigner-Jordan transformation which maps the problem onto a free-fermion system.[16] The role of BC's is then examined. Since this is part of standard techniques we will only show some relevant points. The exact solutions for periodic, antiperiodic, and free-end BC's is then presented. We also discuss the structure of the ground state and the first excited levels.

In Sec. III we perform the numerical calculation for arbitrary tunable BC by diagonalizing the free-fermion Hamiltonian. If we call J_0 the closing bond of the chain prescribed by the BC, and if J is the internal bond in the chain, based on the results presented in this paper, we conjecture a crossover from an exponential behavior of the mass gap to a power law for $g \equiv J_0/J \leq -1$.

Section IV is devoted to the conclusions and final comments.

II. ISING CHAIN WITH TRANSVERSE FIELD AS A FREE FERMION PROBLEM

Our Hamiltonian, including BC effects, is written as follows

$$\hat{\mathcal{H}} = -J \sum_{n=1}^{N-1} \sigma_n^x \sigma_{n+1}^x - J_0 \sigma_N^x \sigma_1^x - \Gamma \sum_{n=1}^{N} \sigma_n^z \ , \tag{3}$$

[where $J>0$ (ferromagnetic exchange), Γ is the transverse field, and the parameter J_0 takes into account the BC's. The reduced constants are defined by

$$\gamma = \frac{\Gamma}{J}, \quad g = \frac{J_0}{J} \ , \tag{4}$$

the cases $g=1$, -1, and 0 corresponding to periodic, antiperiodic, and free-end BC, respectively.

Fermion operators in the chain are defined through the Jordan-Wigner transformation[16] in terms of the spin-ladder operators (σ^+,σ^-):

$$\begin{aligned} C_n &= \exp\left[\pi i \sum_{j=1}^{n-1} \sigma_j^+ \sigma_j^-\right] \sigma_n^- \ , \\ C_n^\dagger &= \sigma_n^+ \exp\left[-\pi i \sum_{j=1}^{n-1} \sigma_j^+ \sigma_j^-\right] \ , \end{aligned} \tag{5}$$

where C_1 is simply σ_1^-. It can be easily found that the total number of fermions is related to the total spin of the chain as follows:

$$\mathcal{N}_c = \sum_{n=1}^{N} C_n^\dagger C_n = \tfrac{1}{2} \sum_{n=1}^{N} (\sigma_n^z + 1) \ . \tag{6}$$

Using the fermion anticommuting rules, the Hamiltonian (3) can be cast to the form

$$\hat{\mathcal{H}}=N\gamma-2\gamma\sum_{n=1}^{N}C_n^\dagger C_n - \sum_{m(<N)}(C_m^\dagger C_{m+1}+C_m^\dagger C_{m+1}^\dagger+\text{H.c.}) +[g\exp(i\pi\mathcal{N}_c)(C_N^\dagger C_1+C_N^\dagger C_1^\dagger)+\text{H.c.}]\ , \tag{7}$$

where we are using reduced unit and H.c. denotes Hermitian conjugate. The presence of the total number of fermions $\mathcal{N}_c$, through the sign operator $\exp(i\pi\mathcal{N}_c)$, makes the problem dependent on the parity of the states except for the particular case $g=0$ (free-end boundaries). The bilinear Hamiltonian (7) can be diagonalized using a standard canonical transformation.[16] Note that parity is conserved since the sign operator $\exp(i\pi\mathcal{N}_c)$ commutes with the total Hamiltonan (7), indicating that the latter only couples states which are in the same parity manifold (even or odd number of fermions).

Following the procedures described in Ref. 16, we write the Hamiltonian (7) and as a canonical bilinear form

$$\hat{\mathcal{H}}=\sum_{m,n}[C_m^\dagger A_{mn}C_n+\tfrac{1}{2}(C_m^\dagger B_{mn}C_n^\dagger+\text{H.c.})]+N\gamma\ , \tag{8}$$

where A_{mn} is a symmetric matrix given below:

$$(A_{mn})=\begin{pmatrix} -2\gamma & -1 & 0 & \dots & 0 & ge^{i\pi\mathcal{N}_c} \\ -1 & -2\gamma & -1 & 0 & \dots & 0 \\ 0 & -1 & -2\gamma & -1 & \dots & 0 \\ \vdots & & & & & \vdots \\ \vdots & & & & & -1 \\ ge^{i\pi\mathcal{N}_c} & 0 & \dots & \dots & -1 & -2\gamma \end{pmatrix}. \tag{9}$$

The matrix (B_{mn}) is anti-Hermitian due to the anticommuting rules for fermion operators

$$\underline{B}^\dagger=-\underline{B}\ , \tag{10}$$

and since the unitary sign operator is self-adjoint, we get

$$(B_{mn})=\begin{pmatrix} 0 & -1 & 0 & \dots & \dots & -ge^{i\pi\mathcal{N}_c} \\ 1 & 0 & -1 & \dots & & \vdots \\ 0 & 1 & 0 & -1 & \dots & \vdots \\ \vdots & \dots & 1 & \dots & & \vdots \\ \vdots & & & & 0 & -1 \\ ge^{i\pi\mathcal{N}_c} & \dots & \dots & 0 & 1 & 0 \end{pmatrix}. \tag{11}$$

In order to diagonalize the Hamiltonian (8) we try the canonical linear transformation below

$$\eta_k\equiv\sum_n(g_{kn}C_n+h_{kn}C_n^\dagger)\ , \qquad \eta_k^\dagger=\sum_n(g_{kn}C_n^\dagger+h_{kn}C_n)\ , \tag{12}$$

where the coefficients g and h are taken as real. The new operators $(\eta,\eta^\dagger)$ preserve the fermion anticommuting relations and reduce Hamiltonian (7) to the simple bilinear form

$$\hat{\mathcal{H}}=\sum_k(\Lambda_k\eta_k^\dagger\eta_k-\tfrac{1}{2}\Lambda_k)\ , \tag{13}$$

where the modes, labeled by the index k, are determined according to the given BC. The eigenvalue problem is better described in terms of the functions

$$\phi_n^{(k)}\equiv g_{kn}+h_{kn}\ , \qquad \psi_n^{(k)}\equiv g_{kn}-h_{kn}\ , \tag{14}$$

which together with definitions (9) and (11) of the $\underline{A}$ and $\underline{B}$ matrices, determine the spectrum as solutions of the equations

$$\Lambda_k\boldsymbol{\phi}^{(k)}=\boldsymbol{\psi}^{(k)}(\underline{A}+\underline{B})\ , \qquad \Lambda_k\boldsymbol{\psi}^{(k)}=\boldsymbol{\phi}^{(k)}(\underline{A}-\underline{B})\ . \tag{15}$$

For $\Lambda_k\neq0$, the above equations are equivalent to the eigenvalue problem

$$\Lambda_k^2\boldsymbol{\phi}^{(k)}=\boldsymbol{\phi}^{(k)}(\underline{A}-\underline{B})(\underline{A}+\underline{B})\ , \tag{16a}$$

$$\Lambda_k^2\boldsymbol{\psi}^{(k)}=\boldsymbol{\psi}^{(k)}(\underline{A}+\underline{B})(\underline{A}-\underline{B})\ . \tag{16b}$$

For arbitrary BC, we have solved numerically the two equations (16), which implies numerical diagonalization of a $(N\times N)$ matrix. If we determine a symmetric matrix $\underline{G}$ as

$$\underline{G}\equiv(\underline{A}-\underline{B})(\underline{A}+\underline{B})\ , \tag{17}$$

its representation (taking into account the proper BC) is given by

$$(G_{nm})=\begin{pmatrix} 4\gamma^2+4g^2 & 4\gamma & 0 & \dots & \dots & -4\gamma ge^{i\pi\mathcal{N}_c} \\ 4\gamma & 4\gamma^2+4 & 4\gamma & \dots & & 0 \\ 0 & 4\gamma & 4\gamma^2+4 & 4\gamma & \dots & 0 \\ \vdots & & & & & \vdots \\ \vdots & & & & & 4\gamma \\ -4\gamma ge^{i\pi\mathcal{N}_c} & 0 & \dots & 0 & 4\gamma & 4\gamma^2+4 \end{pmatrix}. \tag{18}$$

We turn ourselves to the discussion of the exact solutions for periodic (P), antiperiodic (AP), and free-end (FE) BC. In order to get a better insight concerning the structure of the ground state, we will transform to Fourier components of fermion operators, as an intermediate step for transformation (12). We introduce the transformation:[18]

$$C_n=\frac{1}{\sqrt{N}}\sum_k e^{ikn}b_k \ , \tag{19}$$

where the allowed k wave numbers are determined using the appropriate BC. Substitution of transformation (19) into Hamiltonian (7) partially decouples the problem, leaving a single $(k,-k)$ mode coupling, for $-\pi\le k<\pi$. The modes $k=0,-\pi$ have no counterparts and have to be considered separately. Complete diagonalization is attained by the canonical transformation

$$\begin{aligned} b_{-k}&=(\cos\theta_k)\eta_{-k}+i(\sin\theta_k)\eta_k^\dagger \ , \\ b_k^+&=(\cos\theta_k)\eta_k^\dagger+i(\sin\theta_k)\eta_{-k} \ , \end{aligned} \tag{20}$$

where the angle θ_k is determined by the equation

$$\tan(2\theta_k)=\frac{\sin k}{\gamma+\cos k} \ . \tag{21}$$

For the special modes $k=-\pi$, 0, the transformation (20) reduces to

$$\begin{aligned} b_0&=-i\eta_0^\dagger \ , \\ b_{-\pi}&=-i\eta_\pi^\dagger \ , \end{aligned} \tag{22}$$

where for the η operators the modes run over the interval $-\pi<k\le\pi$. The η operators of relation (20) are fermion-like and are the same defined by (12) and (13). The above relations [(12), (13), and (20)] imply that the ground state is doubly occupied by $(k,-k)$ pairs, except when the modes $k=\pi,0$ are allowed. The structure of the ground state $|\mathrm{GS}\rangle$ is then very similar to the Bardeen-Cooper-Schrieffer (BCS) ground state for superconductivity,[18] obtained as the tensor product of states of the form

$$[\cos\theta_k-i(\sin\theta_k)b_k^\dagger b_{-k}^\dagger]\,|0\rangle \ , \tag{23}$$

where $|0\rangle$ denotes the fermion vacuum, and is the ground state and, in turn, the vacuum for the particle excitations defined through the η operators

$$\eta_k\,|\mathrm{GS}\rangle=0 \ , \tag{24}$$

for all k. Since the η operator changes by one the number of fermions we get

$$e^{i\pi\mathcal{N}_c}\eta_k e^{i\pi\mathcal{N}_c}=-\eta_k \ , \tag{25}$$

and when this condition is applied to the definition (24) for the GS, we see that it has a well-defined parity, i.e.,

$$e^{i\pi\mathcal{N}_c}\,|\mathrm{GS}\rangle=\pm\,|\mathrm{GS}\rangle \ . \tag{26}$$

As a product of transformation (20) we get the particle-excitation energy Λ_k as given by

$$\Lambda_k=2(1+\gamma^2+2\gamma\cos k)^{1/2} \ , \tag{27}$$

where the excitation energy of modes $k=0,\pi$, when allowed, are

$$\begin{aligned} \Lambda_0&=2(\gamma+1) \ , \\ \Lambda_\pi&=2(\gamma-1) \ . \end{aligned} \tag{28}$$

As an interesting fact we note that the energy of mode $k=\pi$ changes sign at $\gamma_c=1$, and becomes unstable for $\gamma<1$.[14] This particular mode will drive the phase transition in the limit $N\to\infty$ for the PBC, as we will show below. The value $\gamma_c=1$ happens to be the critical point of the infinite system.

A. Periodic and antiperiodic BC ground state

The allowed k modes are determined through the equations (see Appendix B)

$$\sin(kN)=0, \quad \cos(kN)=-ge^{i\pi\mathcal{N}_c} \ . \tag{29}$$

The parity of the ground state is given by N and we distinguish the cases of even and odd N.

1. *N is even*

For periodic BC, we obtain the modes

$$k_\mathrm{P}=\pm\frac{\pi}{N},\pm\frac{3\pi}{N},\ldots,\pm\frac{(N-1)}{N}\pi \ . \tag{30a}$$

For antiperiodic BC the modes $k=0,\pi$ are occupied:

$$k_\mathrm{AP}=0,\pm\frac{2\pi}{N},\pm\frac{4\pi}{N},\ldots,\pm\frac{N-2}{N}\pi,\pi \ . \tag{31a}$$

2. *N is odd*

Periodic BC yields the result

$$k_\mathrm{P}=0,\pm\frac{2\pi}{N},\pm\frac{4\pi}{N},\ldots,\pm\frac{N-1}{N}\pi \ , \tag{30b}$$

since the mode $k=0$ occupied, but not $k=\pi$.

Antiperiodic BC for N odd yields in turn

$$k_\mathrm{AP}=\pm\frac{\pi}{N},\pm\frac{3\pi}{N},\ldots,\pm\frac{N-2}{N}\pi,\pi \ , \tag{31b}$$

since the particular mode $k=\pi$ occupied but not $k=0$.

We note that the GS is the vacuum for the η-particle excitations (no η-particle states are occupied), and thus the GS energy is given by [see Eq. (13)]

$$E_0=-\tfrac{1}{2}\sum\Lambda_k \ , \tag{32}$$

where the sum is over all allowed k modes.

We also note that Eqs. (30) and (31) can be written in a more compact form if we map the $-\pi<k\le\pi$ Brillouin zone onto the $0\le k<2\pi$ interval [with this scheme however, the elegant representation (23) for the GS is changed somewhat, but the alternative representation given by Eqs. (14)–(16) will suffer no change], being that this representation is the same as that used by Hamer and Barber.[15]

For periodic BC we then get the modes

$$k_\mathrm{P}=\frac{m\pi}{N} \ , \tag{33}$$

for any N, and m being any *odd number* for the interval

$$0 \leq m \leq 2N-1 \ , \tag{34}$$

and the GS energy for periodic BC is given by

$$E_0^{\mathrm{P}} = -\sum_{\substack{m=0 \\ (m \text{ odd})}}^{2N-1} \left[(1-\gamma)^2 + 4\gamma \sin^2 \left[\frac{m\pi}{2N} \right] \right]^{1/2} , \tag{35}$$

which is the same formula given by Hamer and Barber[15] for $\gamma > 1$.

For antiperiodic BC in turn we get the result

$$k_{\mathrm{AP}} = \frac{m\pi}{N} \ , \tag{36}$$

but now m is any *even* number in the interval $0 \leq m \leq 2N-1$. The GS energy in this case is given by

$$E_0^{\mathrm{AP}} = -\sum_{\substack{m=0 \\ (m \text{ even})}}^{2N-1} \left[(1-\gamma)^2 + 4\gamma \sin^2 \left[\frac{m\pi}{2N} \right] \right]^{1/2} . \tag{37}$$

B. Ground state for free-end BC

The allowed k-modes for FEBC are determined through the equation

$$\frac{\sin[k(N+1)]}{\sin(kN)} = -\frac{1}{\gamma} \ , \tag{38}$$

which yields all possible *real* solutions in the interval $0 < k < \pi$. For this particular case, localized states are possible[14] and they are related to complex k numbers. If we explore this possibility we find that there is a complex solution of (38): $k = k_0 + ik_1$, where $k_0 = \pi$, and the imaginary part is obtained through

$$\frac{\sinh[k_1(N+1)]}{\sinh(k_1 N)} = \frac{1}{\gamma} \ . \tag{39}$$

Solutions of Eq. (39) only exist if $\gamma < \gamma_c(N)$, where

$$\gamma_c(N) = \frac{N}{N+1} \ . \tag{40}$$

This localized solution monitors the phase transition of the infinite system, $\gamma_c(N)$, an indication of the critical value:

$$\lim_{N \to \infty} \gamma_c(N) = 1 \ . \tag{41}$$

The energy Λ_k associated with the localized state is given by

$$\Lambda(k_0 + ik_1) = 2(1 + \gamma^2 - 2\gamma \cosh k_1)^{1/2} \ , \tag{42}$$

and this is the first particle excitation in the spectrum (i.e., it determines the energy gap). The asymptotic expression of (39), for $N \to \infty$, is given by

$$e^{k_1} = \frac{1}{\gamma} \ , \tag{43}$$

for $\gamma < 1$, and the corresponding solution

$$k_1 = -\ln\gamma \ , \tag{44}$$

is exactly the expression for the surface tension of the 1D Ising model with transverse field (see Ref. 12).

C. Excitation spectrum

When dealing with PBC's and APBC's special care has to be taken for the excited states which have a different parity than those of the corresponding ground states (states with odd number of η-particle excitations). The above mentioned states are defined in relation to a "virtual" ground state whose parity is minus the parity of the true ground state. Thus the "virtual" GS for PBC corresponds to the true GS for APBC (and vice versa), indicating that the odd-particle excitations are defined in relation to a modified Fermi sea.

The first excited state for PBC is then given by

$$E_1^{\mathrm{P}} = 2(\gamma-1) - \sum_{\substack{m=0 \\ (m \text{ even})}}^{2N-1} \left[(1-\gamma)^2 + 4\gamma \sin^2 \left[\frac{m\pi}{2N} \right] \right]^{1/2} , \tag{45}$$

which follows from formulae (28), (37), and (13). It is worth remarking that $\Lambda_\pi = 2(\gamma-1) < 0$ for $\gamma < 1$, implying that the energy gap will vanish with increasing size for $\gamma < 1$.

For APBC the first excited state is *two-fold degenerate*, corresponding to one-particle excitations with wave numbers $k = (\pi/N), (2N-1/N)\pi$

$$E_1^{\mathrm{AP}} = 2\left[(1-\gamma)^2 + 4\gamma \sin^2 \left[\frac{\pi}{2N} \right] \right]^{1/2} - \sum_{\substack{m=0 \\ (m \text{ odd})}}^{2N-1} \left[(1-\gamma)^2 + 4\gamma \sin^2 \left[\frac{m\pi}{2N} \right] \right]^{1/2} , \tag{46}$$

and collecting both together with relations (35) and (37), we obtain

$$\begin{aligned} E_1^{\mathrm{P}} &= 2(\gamma-1) + E_0^{\mathrm{AP}} \ , \\ E_1^{\mathrm{AP}} &= 2\left[(1-\gamma)^2 + 4\gamma \sin^2 \left[\frac{\pi}{2N} \right] \right]^{1/2} + E_0^{\mathrm{P}} \ , \end{aligned} \tag{47}$$

indicating that there is a simple relation linking the mass gap for both cases. Defining

$$\begin{aligned} m^{\mathrm{P}}(N;\gamma) &\equiv E_1^{\mathrm{P}} - E_0^{\mathrm{P}} \ , \\ m^{\mathrm{AP}}(N;\gamma) &\equiv E_1^{\mathrm{AP}} - E_0^{\mathrm{AP}} \ , \end{aligned} \tag{48}$$

from relations (47), we obtain

$$m^{\mathrm{AP}}(N;\gamma) = 2\left[(1-\gamma)^2 + 4\gamma \sin^2 \left[\frac{\pi}{2N} \right] \right]^{1/2} + 2(\gamma-1) - m^{\mathrm{P}}(N;\gamma) \ . \tag{49}$$

For FEBC's the modes are always the same, given as solutions of Eq. (38), and the mass gap is always determined by the wave number whose real part k_0 is closer to π.

(i) For $\gamma > \gamma_c = N/(N+1)$ this wave number is real and the mass gap converges to $2(\gamma-1)$ for $N \to \infty$.

(ii) For $\gamma < \gamma_c$, the mass-gap is determined by the localized excitation with complex $k_0 + ik_1$ wave number, where $k_0 = \pi$ and k_1 is solution of Eq. (39). In this case the mass-gap vanishes in the limit $N \to \infty$.

Asymptotic expressions for the mass gap can be obtained straightforwardly. In this paper our attention is focused on the case $\gamma < 1$, which is asymptotically degenerate for $N \to \infty$. Following the prescriptions given by Barber and Fisher for the spherical model,[2] the mass gap for the PBC can be written asymptotically as

$$m^{\mathrm{P}}(N;\gamma) \underset{N\to\infty}{\cong} 2\left[\frac{1-\gamma^2}{\pi}\right]^{1/2} \frac{\gamma^N}{N^{1/2}} \quad (\gamma < 1) , \tag{50}$$

i.e., it converges exponentially to zero with increasing size. Using relation (49) we can obtain the asymptotic expression for APBC

$$m^{\mathrm{AP}}(N;\gamma) \underset{N\to\infty}{\cong} \frac{\gamma\pi^2}{1-\gamma}\left[\frac{1}{N^2}\right] \quad (\gamma < 1) , \tag{51}$$

which shows that there is a drastic change in the way the system goes to the thermodynamic limit.

Concerning the FE case, the development for $N \to \infty$ yields

$$m^{\mathrm{FE}}(N;\gamma) \underset{N\to\infty}{\cong} 2(1-\gamma^2)\gamma^N \quad (\gamma < 1) , \tag{52}$$

where an exponential convergence to zero is also obtained but this convergence is weaker than the case of PBC by a factor $N^{1/2}$.

Other excited states for all the cases are built in a similar way as the one described here. For P and APBC, states with even number of excitations use the "true" GS as a reference for selecting the modes.

For FEBC, the phase transition when $N \to \infty$ is due to a particular excitation which localizes itself on both free "surfaces" (see the Appendix).

For arbitrary BC we were not able to find exact analytical solutions (see Appendix B). We have then turned to numerical diagonalization of the Jordan-Wigner matrix (18) as a function of the size. Note that the fermion representation significantly reduces the dimensionality of the problem, when compared to the original spin representation. The results of this calculation are presented in the next section.

We end this section with a final comment concerning the asymptotic expressions (50) to (52). The lack of universality of the mass-gap size dependence can already be seen from these relations. The exponential behavior $\exp(-\sigma N)$, with $\sigma = \ln\gamma$, is only obtained for P and FEBC. Even in this case, the prefactor of the exponential is different, being the convergence stronger (with an extra factor $N^{-1/2}$) for PBC. This means that PBC simulate better the bulk behavior, as expected from intuitive grounds.

A striking crossover to a power law is obtained for APBC—see formula (51)—the excitation spectrum being in this case double degenerate. In the next section we numerically interpolate between the above behavior for arbitrary BC.

III. NUMERICAL CALCULATION FOR ARBITRARY BC

For arbitrary BC we have performed numerically the diagonalization of matrix (18). This process yields the eigenvalues which determine the spectrum of the fermion Hamiltonian. Simultaneously we have also numerically diagonalized the $2^N \times 2^N$ matrix corresponding to the original spin Hamiltonian given by (3) for small sizes (up to $N = 8$). In this way a systematic check of our results have been made to warrant the right choice of the eigenvalues for the fermion problem. Since the G matrix defined by (3) has dimension N, larger sizes can be attained and the main limitation in accuracy comes from the weakness of the mass gap itself, specially when its dependence on size is exponential. High precision can be obtained near criticality (i.e., for γ close to 1), and in the range $g \le -1$, where the mass-gap behavior is given by a power law (sizes of the order of $N \approx 100$ can be easily reached).

The asymptotic dependence for very large N has been assumed to be of the form

$$m(N) = AN^{-\alpha}\exp(-\sigma N) , \tag{53}$$

where the quantities α and σ can generally depend on γ and on the BC through the g parameter.

As usual in finite-size scaling calculations we define size-dependent quantities[12]

$$\begin{aligned} X(N) &\equiv \ln\left[\frac{N}{N-1}\right] , \\ Y(N) &\equiv \ln\left[\frac{m(N)}{m(N-1)}\right] , \end{aligned} \tag{54}$$

which would be linearly related for large N if relation (53) is satisfied. The slope of the asymptotic regime gives the exponent α, while the coefficient σ will be the ordinate at the origin. For efficient extrapolation, size-dependent quantities are also defined

$$\alpha(N) \equiv -\left[\frac{Y(N)-Y(N-1)}{X(N)-X(N-1)}\right] , \tag{55}$$

$$\sigma(N) \equiv -Y(N) + \alpha(N)X(N) . \tag{56}$$

From definitions (54) to (56) it follows that $\alpha(N)$ and $\sigma(N)$ are calculated from data corresponding to three successive sizes, $N-2$, $N-1$, and N. The exponent α and the coefficient σ (known as the anisotropic limit of the surface tension) of formula (53) can be estimated from extrapolation for $N \to \infty$, if convergence for the quantities $\alpha(N)$ and $\sigma(N)$ is obtained.

Typical results of the above described calculation are depicted in Figs. 1 and 2, where we illustrate two cases exactly calculated in the preceding section (FE and APBC). For the FEBC case we get an asymptotic exponential behavior, being the convergence of $\sigma(N)$ to its asymptotic value $-\ln\gamma$ quite good. The quantity $\alpha(N)$ converges very quickly to zero in agreement with the ex-

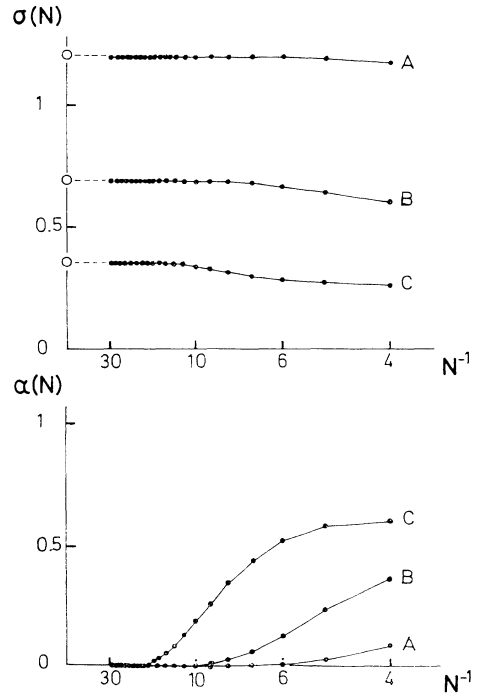

FIG. 1. Plots of $\sigma(N)$ and $\alpha(N)$ as functions of N^{-1} for $g=0$ (FEBC). The curves A, B, and C correspond to $\gamma=0.3$, 0.5, and 0.7, respectively. The exact results $\sigma=-\ln\gamma$ are indicated by open circles.

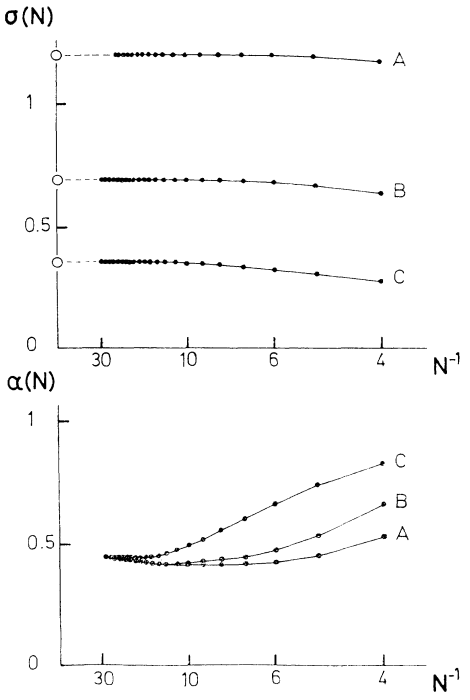

FIG. 3. Plots of $\sigma(N)$ and $\alpha(N)$ as functions of N^{-1} for $g=0.5$. The curves A, B, and C correspond to $\gamma=0.3$, 0.5, and 0.7, respectively. The exact results $\sigma=-\ln\gamma$, valid for FEBC, are indicated by open circles.

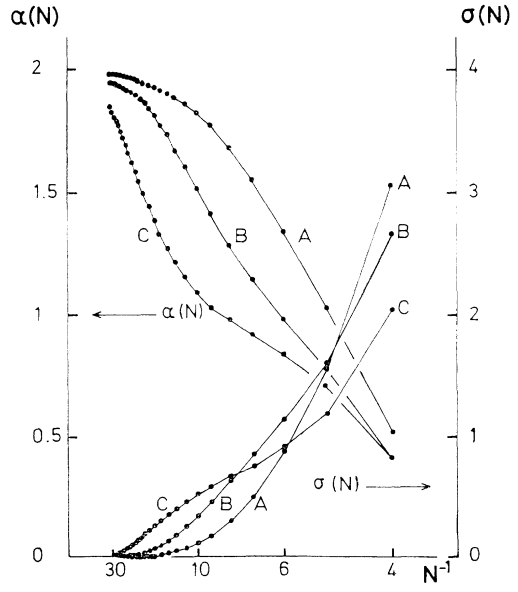

FIG. 2. Plots of $\sigma(N)$ and $\alpha(N)$ as function of N^{-1} for $g=-1$ (APBC). The curves A, B, and C correspond to $\gamma=0.3$, 0.5, and 0.7, respectively.

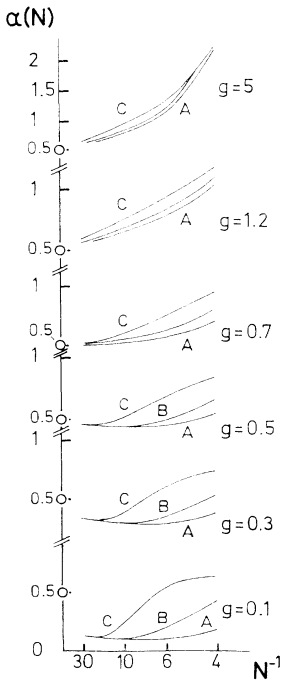

FIG. 4. Plots of $\alpha(N)$ as functions of N^{-1} for different positive g values, decreasing from $g=5.0$ down to $g=0.1$. In each case, the curves A, B, and C correspond to $\gamma=0.3$, 0.5, and 0.7, respectively.

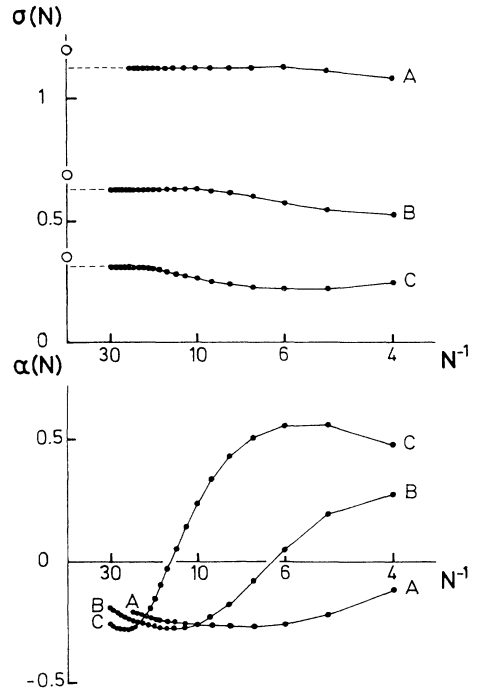

FIG. 5. Plots of $\sigma(N)$ and $\alpha(N)$ as functions of N^{-1} for $g=-0.3$. The curves A, B, and C correspond to $\gamma=0.3$, 0.5, and 0.7, respectively. The exact results $\sigma=-\ln\gamma$, valid for FEBC, are indicated by open circles.

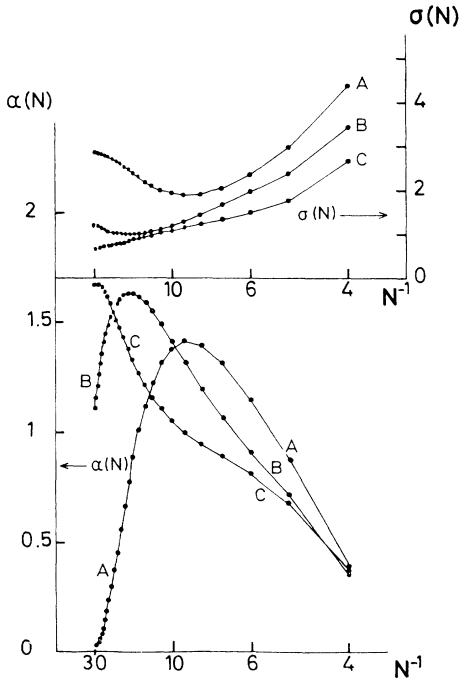

FIG. 7. Plots of $\sigma(N)$ and $\alpha(N)$ as functions of N^{-1} for $g=-0.9$. The curves A, B, and C correspond to $\gamma=0.3$, 0.5, and 0.7, respectively.

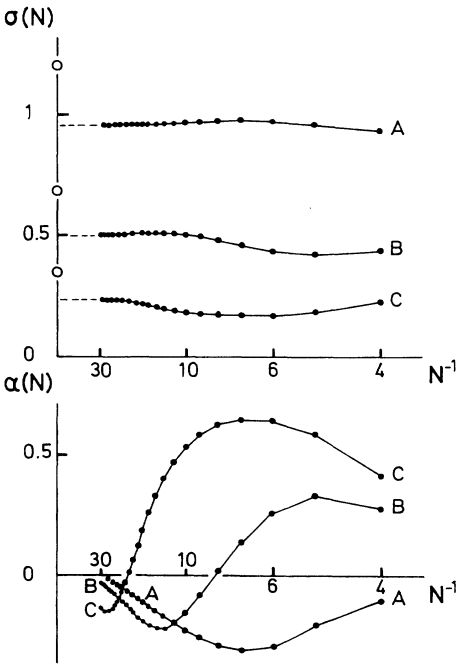

FIG. 6. Plots of $\sigma(N)$ and $\alpha(N)$ as functions of N^{-1} for $g=-0.5$. The curves A, B, and C correspond to $\gamma=0.3$, 0.5, and 0.7, respectively. The exact results $\sigma=-\ln\gamma$, valid for FEBC, are indicated by open circles.

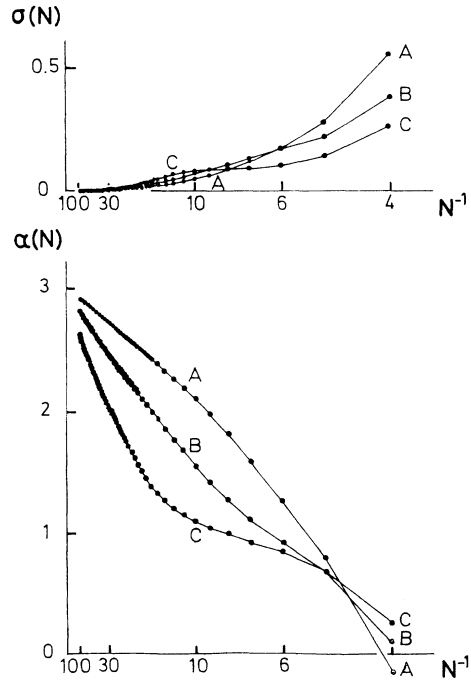

FIG. 8. Plots of $\sigma(N)$ and $\alpha(N)$ as functions of N^{-1} for $g=-1.5$. The curve A, B, and C correspond to $\gamma=0.3$, 0.5, and 0.7, respectively.

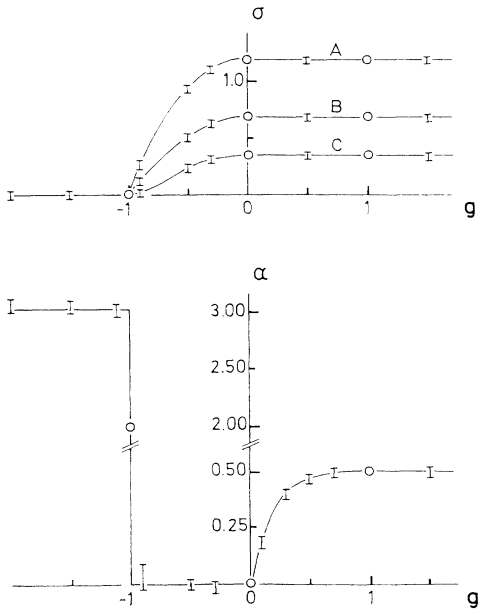

FIG 9. Summary of the results for the extrapolated values of σ and α as function of the parameter g. The exact results are indicated by the circles and the numerical results are indicated by the error bars.

act asymptotic exponent $\alpha=0$. Concerning APBC (Fig. 2) the numerical result shows neatly the power-law asymptotic behavior of the mass gap with $\alpha=2$ and $\sigma=0$. Numerical results for PBC were already presented in Ref. 12, where small-size calculations already showed a good convergence to the values $\sigma=-\ln\gamma$ and $\alpha=\frac{1}{2}$. Those values were verified here with much more accuracy for larger sizes, in complete agreement with formula (50).

For arbitrary BC, as long as $g\geq 0$, a leading exponential behavior for the mass gap is always found. Convergence to the value $\sigma=-\ln\gamma$ is quick as shown in Fig. 3 for the case $g=0.5$. The situation for the prefactor of the exponential is more complex. The size-dependent quantity $\alpha(N)$ seems to converge to values which continuously interpolate between the value $\alpha=\frac{1}{2}$ for PBC and $\alpha=0$ for FEBC. In some cases, up to sizes of the order of $N\approx 30$, extrapolation for $N\to\infty$ is still difficult. For $g>1$ the value of α, with good accuracy, saturates to the PBC value $\alpha=\frac{1}{2}$. A series of a calculation of $\alpha(N)$ for $g>0$ is shown in Fig. 4 for various values of $\gamma<1$, displaying the sensibility of α with BC.

The situation is even more interesting for $-1<g<0$, where we also obtain a variation of σ, as shown in Figs. 5–7. The $\alpha(N)$ quantity becomes negative in some cases, and for values close to $g=-1$ from above, we find a crossover from an apparent values $\alpha\approx 2$ for small sizes to $\alpha\approx 0$ for much larger sizes (see Fig. 7). Size effects are strong in this case yielding to uncertainties in the extrapolated values.

For $g\leq -1$ we have a striking phenomenon: The exponential convergence stops and is replaced by a power law. Exact and numerical calculations yield the exponent $\alpha=2$ for $g=-1$ (APBC) and very accurate large-size calculations extrapolates to $\alpha\approx 3$ for $g<-1$. *It is impressive and puzzling to see that convergence ceases as a result of boundary effects.* Are we creating for $g\leq -1$ a topological defect? If the boundary spins are antiferromagnetically pinned by the BC, our system will have the topology of a Möbius strip, being the excitation spectrum radically different from that for $g>0$. Indeed, the low-lying excitations will correspond to odd number of kinks (Bloch walls) instead of pairs of kinks and antikinks, as it is the case for regular periodic BC.[19] In Fig. 8 we are displaying the case of $g=-1.5$, and Fig. 9 is a summary of all of our results for both σ and α as a function of g, for various values of the transverse field.

IV. CONCLUSIONS

For the original Hamilton (3) we define a "kink operator" by

$$\hat{O}_n \equiv \prod_{m>n} \sigma_m^z \ . \tag{57}$$

When acting over a completely ordered state, this operator $\hat{O}_n$ flips all the spins to the right of site n, creating a kink excitation or Bloch wall. For the low-temperature phase ($\gamma<1$), kink states interpolate between the ground state and the first excited level[19] (the one which defines the mass gap). It is clear that there is a close relation between the structure of kink excitations and BC, having this relation topological relevance. Work is under progress to elucidate the role of kink excitations on the size dependence of the mass gap. One other interesting point suggested by our results is aimed at the calculation of the surface tension for the isotropic 2D Ising model in the presence of variable BC.[20]

Finally, we note that scaling functions are strongly dependent on BC whether at criticality[2,4] or not. Universality has then a restricted meaning when dealing with finite-size scaling. For the Ising model, as long as the BC are varied, the regular exponential convergence strikingly changes in a much weaker power-law behavior. We suggest that this crossover is related to a topological defect associated to the strong antiferromagnetic coupling between the boundaries.

ACKNOWLEDGEMENTS

We would like to acknowledge stimulating discussions with P. Pfeuty, E. Brézin, J. Zinn-Justin, and M. Kolb. One of the authors (G.G.C.) also acknowledges helpful conversations with L. M. Falicov. The Brazilian part of this work was partially supported by the Brazilian agencies CNPq and FAPESP. The numerical calculations were done at CIRCE (Centre Interrégional de Calculs Electroniques), Orsay.

APPENDIX A

For FEBC the exact solution of Eq. (16a), for the localized mode k_0+ik_1 (with $k_0=\pi$) is given by

$$\phi_m = A_N(-1)^{m-1}\sinh[(N-m+1)k_1] \ , \tag{A1}$$

where $m=1,2,\ldots,N$ and A_N is a normalization factor:

$$A_N = \frac{i^{2N+1}(2\sinh k_1)^{1/2}}{\{\sinh(Nk_1)\cosh[(N+1)k_1]-N\sinh k_1\}^{1/2}} \ . \quad \text{(A2)}$$

The corresponding ψ_m functions defined by (14) can be obtained through relation (15). We obtain

$$\psi_m = [2A_N(-1)^m/m(N)]\{\gamma\sinh[(N-m+1)k_1] - \sinh[(N-m)k_1]\} \ , \quad \text{(A3)}$$

where $m(N)$ is the mass gap for FEBC. In the asymptotic limit, for N very large, ϕ represents essentially a state localized at site $m=1$, and decays exponentially to the interior of the chain with a factor $\exp(-k_1)$. Asymptotically we have, for $N\to\infty$,

$$k_1 \to \sigma = -\ln\gamma \ , \quad \text{(A4)}$$

for $\gamma<1$. On the other hand ψ represents a state essentially localized at the other chain extreme, with the same decaying factor.

If $\eta^\dagger$ is the canonical creation operator associated to the localized mode we have

$$\eta^\dagger = \sum_{m=1}^{N} (g_m c_m^\dagger + h_m c_m) \ , \quad \text{(A5)}$$

where g_m and h_m are related to ϕ_m and ψ_m through relation (14), i.e.,

$$g_m = \tfrac{1}{2}(\phi_m+\psi_m) \ ,$$

$$h_m = \tfrac{1}{2}(\phi_m-\psi_m) \ .$$

It is then clear that the operator $\eta^\dagger$, in the limit of very large N, only modifies the ground state at both chain extremes.

APPENDIX B

If we denote by P the sign operator $\exp(i\pi\mathcal{N}_c)$, the solutions of the eigenvalue Eq. (16a), with the G matrix given by (18), satisfy the linear equations

$$\begin{aligned}
&(4\gamma^2+4g^2-\lambda_k)\Phi_1^{(k)}+4\gamma\Phi_2^{(k)}-4g\gamma P\Phi_N^{(k)}=0 \ ,\\
&4\gamma\Phi_1^{(k)}+(4\gamma^2+4-\lambda_k)\Phi_2^{(k)}+4\gamma\Phi_3^{(k)}=0 \ ,\\
&4\gamma\Phi_{N-2}^{(k)}+(4\gamma^2+4-\lambda_k)\Phi_{N-1}^{(k)}+4\gamma\Phi_N^{(k)}=0 \ ,\\
&4\gamma\Phi_{N-1}^{(k)}+(4\gamma^2+4-\lambda_k)\Phi_N^{(k)}-4g\gamma P\Phi_1^{(k)}=0 \ .
\end{aligned} \quad \text{(B1)}$$

General solutions of (B1) are given by

$$\Phi_m^{(k)} = A\sin(km)+B\cos(km) \ , \quad \text{(B2)}$$

with the eigenvalues

$$\lambda_k = \Lambda_k^2 = 4(\gamma^2+1+2\gamma\cos k) \ , \quad \text{(B3)}$$

The BC's determine the choice of the k modes through the secular equation given below:

$$(g^2-1)\left[\frac{\sin(kN)}{\sin k}+g(1-P)\cos k\right] + \gamma\left[g^2\frac{\sin[k(N-1)]}{\sin k} - \frac{\sin[k(N+1)]}{\sin k} - 2gP\right]=0 \ . \quad \text{(B4)}$$

The equations (29) and (38) in the main text are particular cases of (B4). For instance, P and APBC. In this case $g^2=1$, and we obtain

$$\gamma[\cos(kN)+gP]=0 \ ,$$

or equivalently

$$\cos(kN) = -gP \ .$$

For FEBC we have $g=0$, and then

$$\frac{\sin(kN)}{\sin k}+\gamma\frac{\sin[k(N+1)]}{\sin k}=0 \ ,$$

or

$$\frac{\sin[k(N+1)]}{\sin(kN)} = -\frac{1}{\gamma} \ .$$

---

*Permanent address.

[1]L. A. Kolodziejski, R. L. Gunshor, N. Otsuka, B. P. Gu, Y. Hefetz, and A. V. Nurmikko, Appl. Phys. Lett. **48**, 1482 (1986).

[2]M. N. Barber and M. E. Fisher, Ann. Phys. **77**, 1 (1973).

[3]M. N. Barber, in *Phase Transitions and Critical Phenomena,* edited by C. Domb and J. Lebowitz (Academic, New York, 1984), Vol. VIII, p. 146.

[4]T. W. Burkhardt and I. Guim, J. Phys. A **18**, L33 (1985).

[5]G. G. Cabrera and R. Jullien, Phys. Rev. Lett. **57**, 393 (1986).

[6]M. Suzuki, Prog. Theor. Phys. **46**, 1337 (1971); **56**, 1454 (1976); E. Fradkin and L. Susskind, Phys. Rev. D **17**, 2637 (1978); J. B. Kogut, Rev. Mod. Phys. **51**, 659 (1979).

[7]Modern theory of critical phenomena assumes that statistical systems at a critical point are not only scale invariant, but also conformally invariant. For conformal symmetry and second-order phase transitions, see A. Z. Patashinskii and V. L. Pokrovskii, *Fluctuation Theory of Phase Transitions* (Pergamon, Oxford, 1979), p. 55.

[8]M. E. Fisher, in *Critical Phenomena,* Proceedings of the "Enrico Fermi" Summer School, Course LI Varenna, edited by M. S. Green (Academic, New York, 1971); M. E. Fisher and M. N. Barber, Phys. Rev. Lett. **28**, 1516 (1972).

[9]M. P. Nightingale, Physica **83**, A561 (1976).

[10]V. Privman and M. E. Fisher, J. Stat. Phys. **33**, 385 (1983).

[11]E. Brézin and J. Zinn-Justin, Nucl. Phys. B **257**, 867 (1985).

[12]G. G. Cabrera, R. Jullien, E. Brézin, and J. Zinn-Justin, J. Phys. (Paris) **47**, 305 (1986).

[13]J. L. Cardy, J. Phys. A **17**, L385 (1984).

[14]P. Pfeuty, Ann. Phys. (N.Y.) **57**, 79 (1970).

[15]C. J. Hamer and M. N. Barber, J. Phys. A **14**, 241 (1981).

[16]E. Lieb, T. Schulz, and D. Mattis, Ann. Phys. (N.Y.) **16**, 407

(1961).
[17]M. E. Fisher, J. Phys. Soc. Jpn. Suppl. **26**, 87 (1969).
[18]D. C. Mattis, *The Theory of Magnetism II: Thermodynamics and Statistical Mechanics* (Springer-Verlag, Berlin, 1985), p. 112.
[19]The relation between kink excitations and topology is discussed in the review article by J. B. Kogut in Ref. 6 in the present paper.
[20]J. Zinn-Justin has recently made a comment where he suggests how to calculate the variation of σ with different BC. For the 2D Ising model the dominant configuration contributing to the correlation length corresponds to an interface which rotates as long as BC are varied [Phys. Rev. Lett. **57**, 3296 (1986)].